Experiments in Fluids 13, 257–266 (1992)

Experiments in Fluids

The periodicity of droplets emanating from interconnected orifices

D. M. Weis, P. F. Dunn and **M. Sen**

Department of Aerospace and Mechanical Engineering, University of Notre Dame, Notre Dame, IN 46556, USA

Abstract. The periodicity of droplets emanating from a single and from two orifices with a common fluid reservoir between them was investigated. Experiments were conducted in which the effects of variations in mass flow rate, orifice diameter and common reservoir volume were determined. The results reported herein indicate that dripping from an orifice at relatively low mass flow rates is singly periodic and that the period between droplets is inversely proportional to the imposed mass flow rate. A simple model of the singly periodic droplet emission process is developed and supported by the experimental results. Period doubling initiates and continues to develop with further increases in the mass flow rate. It is marked by the introduction of additional, smaller diameter droplets that are interspersed temporally among the larger, primary droplets. The presence of a common fluid reservoir volume between two orifices of the same diameter is shown for the singly periodic regime not to alter the droplet emission rate of either orifice as compared to its single orifice counterpart. The volume of the reservoir, however, does affect the mass flow rate per orifice necessary for initial period doubling, with this mass flow rate being lower for a smaller reservoir volume.

1 Introduction

There are many devices such as bubble jet printers (Asai 1989) whose operation is based upon the expulsion of liquid from multiple nozzle arrangements that are fed from a common fluid reservoir. In this situation there can be some degree of dynamic interaction between the flow from each orifice. Herein, we report on an experimental study of this type of interaction using the very simplified yet realistic geometries of a single orifice and two orifices with a common fluid reservoir between them. Although a number of studies have been conducted using a single orifice, no similar studies of two common-fluid-reservoir orifices have appeared in the literature.

There are many reports on experiments with the dripping of a liquid from a single small orifice when the period between drops is relatively large, on the order of ten to several hundred seconds. In such quasi-static situations, primarily surface tension and gravitational forces govern droplet formation. One of the earliest investigations was reported in 1864 by Tate, a pharmacist, who performed experiments to quantify the effects of tube diameter and other parameters on the weight of the dispensed droplet. Additional, related studies were reported by Rayleigh (1899), Harkins and Brown (1919), Padday and Pitt (1973), and Wilson (1988). Manfré (1966) presented a model of and experimental results for droplet formation driven by a hydrostatic head and reviewed previous, related works. These studies collectively revealed that the size of a droplet formed from the pendant liquid emanating from an orifice was governed not only by surface tension and gravitational forces but also by the shape of the pendant's neck curvature at the instant of release. This curvature implicitly was related to the dimensions of the orifice and droplet, and the liquid's properties. These studies, however, did not examine either the periodic nature of droplet emission per se or its stability.

Several definite studies on the dynamics of droplet emission from an orifice have been conducted more recently at higher droplet emission rates. These studies have extended from the regime of periodic droplet emission to that of chaotic emission. Shaw (1984), Martien et al. (1985) and Crutchfield et al. (1986), for example, have performed experiments to examine the dynamical aspects of a dripping faucet, including the period-doubling transition to chaotic behavior. They have demonstrated amply that at small flow rates the dripping is periodic, but on increasing the flow rate, period doubling occurs. A further increase in the flow rate led to more bifurcations and eventually to chaotic behavior. In addition, Shaw (1984) presented a simple dynamical system model, which has some of the characteristics of the experimental results. Wu and Schelly (1989) also have carried out experiments with the single orifice to determine the effect of temperature dependent surface tension on the process.

Rather than concentrating on the chaotic aspect of falling drops, the present experiments investigated further the periodic regime and, in particular, the effect that various system parameters had on the periodic behavior of the droplet emission and the interaction between orifices. For a single orifice, like that of Shaw's, the effects of mass flow rate and orifice diameter on droplet periodicity were investigated. Then, using two orifices with a common fluid reservoir

between them, the effect of the reservoir fluid volume was examined. This study differs from previous ones in that the present experiments were conducted at fixed volumetric flow rates, whereas the aforementioned experiments were carried out with the flow being driven by a constant pressure head.

2 Experimental apparatus

A schematic of the system used for the present experiments is shown in Fig. 1. In this configuration, the times of droplet emission from either a single orifice or two interconnected orifices were detected using a laser/photodetector arrangement and the droplet mass flow rate using an electronic balance. Additional details of the experimental apparatus are presented by Weis et al. (1991).

Specifically, liquid ethanol was supplied to the orifice(s) through flexible tubing from a 50 ml plastic syringe mounted on a constant volumetric (therefore, constant mass) flow rate syringe pump. The volumetric flow rate range for the present experiments, from approximately 2 to 20 ml/min, resulted in effluent droplet mass flow rates from approximately 30 to 300 mg/s. The typical duration for an experiment was 2 minutes. The effluent ethanol was collected in a glass beaker placed on top of an electronic balance that recorded the accumulated mass of the droplets with an uncertainty of ± 10 mg. Information on the accumulated droplet mass was gathered in real-time on a personal computer and then used to determine the droplet mass flow rate. For the range of mass flow rates investigated, this yielded maximum uncertainties in the mass flow rate ranging from $\pm 0.03\%$ to $\pm 0.28\%$, assuming a negligible error in the measurement of time. For the double orifice experiments, the mass flow rate from each individual orifice was measured in addition to the total mass flow rate. In this paper, the term mass flow rate refers to the total mass flow rate supplied by the syringe pump, and the term mass flow rate per orifice to that through an individual orifice.

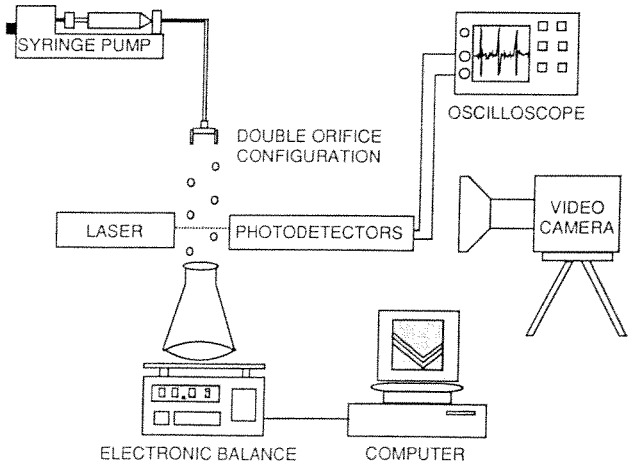

Fig. 1. Schematic of the experimental set-up

A laser/photodetector system was used to detect the time at which droplets departed from the tips of the orifices. The beam from a 10 mW HeNe laser was split and aligned using reflecting mirrors to cross each falling droplet pathway approximately 5 cm below the tips of the orifices. One beam was directed through a half-silvered mirror directly onto a pinhole aperture masking a photomultiplier tube, while the other was reflected by the half-silvered mirror and then a reflecting mirror to a photodiode that was mounted behind another pinhole aperture. The signal from the photomultiplier tube was sent to one channel of a digital oscilloscope. The photodiode was connected in series with a 220 ohm resistor and a constant voltage supply. The voltage drop across this resistor was monitored on another channel of the oscilloscope. In this manner, the photodetectors' responses to the falling droplets that interrupted the laser beams could be viewed simultaneously on the oscilloscope and stored for subsequent analysis. The photodetector system yielded signal-to-noise ratios of approx. 20-to-1, which were easy to discriminate to determine the droplet period. Based on repeated measurements using the time cursors on the oscilloscope to determine the droplet period, the error was determined to be ± 4 ms of 400 ms full scale. Thus, the maximum uncertainty in the droplet period was $\pm 1\%$.

Three different cylindrical, blunt-tip orifices denoted as orifices A, B and C, were utilized in this investigation. Orifice A, used for the majority of the experiments, was a miniature barbed polypropylene 1/16 in. $\times$ 1/16 in. fitting with a tip length = 0.838 ± 0.025 mm, ID = 1.080 ± 0.013 mm, and OD = 1.727 ± 0.025 mm. Orifice B was a 21 gauge stainless steel hypodermic needle with a length = 15.1 ± 0.1 mm, ID = 0.521 ± 0.013 mm, and OD = 0.813 ± 0.013 mm. Orifice C was a stainless steel tubing-to-male Luer needle lock connector with a tip length = 8.5 ± 0.1 mm, ID = 1.867 ± 0.025 mm, and OD = 4.077 ± 0.025 mm. These tolerances resulted in maximum errors in the IDs of $\pm 1.20\%$, $\pm 2.50\%$ and $\pm 1.34\%$ for orifices A, B and C, respectively.

Two double-orifice configurations were utilized for the experiments in which the effect of reservoir volume size was examined. Each configuration was constructed by attaching two A orifices with elbows to a T-shaped junction whose remaining end was connected to a flexible tubing supply line. This configuration is illustrated in Fig. 1. One configuration's (reservoir I) common reservoir volume was approx. 0.014 cm^3; the other's (reservoir II) approx. ten times larger or 0.14 cm^3. Because the droplet diameters ranged from approx. 2 to 3 mm in the present experiments, the reservoir-to-droplet volume ratios ranged from approx. 1:1 to 3:1 for reservoir I, and 10:1 to 30:1 for reservoir II.

The droplet formation process was recorded at 60 frames/sec on VHS video cassette using a video camera with a 12 $\times$ zoom lens. In some instances, a microscopic lens with a 20 $\times$ objective was used in place of the zoom lens to acquire detailed close-ups of the droplets during their formation and after their departure from an orifice. From the images of the detached droplets, using the orifice's OD as a scaling dimen-

sion, the droplet diameters were determined to within ± 0.02 mm. This resulted in a maximum uncertainty in the droplet diameter of approximately $\pm 1\%$.

3 Data analysis methods

For each experiment conducted, at least 100 successive periods were measured from the stored oscilloscope records. The resulting temporal records were analyzed using several methods. This composite approach yielded several unique features of the evolution of droplet emission with increasing flow rate. These methods included plotting the period data in the form of return maps, determining the period data autocorrelation function and constructing the droplet period histogram.

In the experiments of Shaw (1984), the period between successive drops was recorded as $T_1, T_2, T_3 \ldots$ and then examined in T_{n+1} versus T_n plots. This is a map of each period mapping into the next. Similar return maps were constructed here. Perfect periodicity with each successive period equaling the previous one would be characterized by a point on a 45° line extending from the origin. Perfect period doubling would appear as two points on this map, symmetrically located about the 45° line.

For the purpose of examining the correlation functions, a time series, $x(t)$, was constructed consisting of pulses of unit height centered at the time of occurrence and of width Δ. The pulse width Δ was taken to be 10 ms, which is the typical transit time of a droplet through the laser beam. The normalized autocorrelation function of $x(t)$ is then defined by

$$R_x^*(\tau) \equiv \frac{R_x(\tau)}{R_{x,\max}(\tau)} \tag{1}$$

where

$$R_x(\tau) = \lim_{N\to\infty} \frac{1}{N} \int_0^N x(t)\, x(t+\tau)\, \mathrm{d}t\,.$$

In this expression, N denotes the number of event pulses (here ≥ 100). The normalized autocorrelation, $R_x^*(\tau)$, is shown in the figures, with τ being the delay time. The time series of perfectly periodic events would yield an autocorrelation of triangular-shaped pulses, each with a base width of 2Δ, at delay times $\tau = nT$, where $n = \pm 0, 1, 2 \ldots$ and T is the primary period.

For the double orifice data, two time series, $x(t)$ and $y(t)$, were constructed for each orifice. The normalized cross-correlation function, $R_{xy}^*(\tau)$, is defined by

$$R_{xy}^*(\tau) \equiv \frac{R_{xy}(\tau)}{R_{xy,\max}(\tau)} \tag{2}$$

where

$$R_{xy}(\tau) = \lim_{N\to\infty} \frac{1}{N} \int_0^N x(t)\, y(t+\tau)\, \mathrm{d}t\,.$$

Here, two time series with perfect periodic events of periods T_1 and T_2 would yield triangular-shaped pulses, each with a base width of 2Δ, centered at delay times τ when $\tau = nT_1 = mT_2$, where n and $m = \pm 0, 1, 2 \ldots$.

4 Single orifice experiment results and discussion

A series of nine experiments were performed in which the effects of mass flow rate and orifice diameter were investigated. Seven of these were conducted using orifice A, and of the remaining two, one with orifice B and the other with orifice C. An additional experiment using orifice A was performed in which the emitted droplets were recorded on video cassette under high magnification to examine the relation between droplet diameter and period.

4.1 Effect of mass flow rate variation

Seven different mass flow rates, between 30 and 210 mg/s, were chosen to investigate the effect of mass flow rate on the periodicity of the droplet emission. The specific flow rates examined were selected based upon initial observations identifying those at which the evolution of droplet production with increasing flow rate was best characterized. The detailed results of all of the cases examined are presented by Weis et al. (1991). For brevity, the results of only two of the seven cases (116 and 191 mg/s) examined are shown in Fig. 2. These two cases respectively represent the situations before and after period doubling. The return map, autocorrelation and period histogram for each of these two flow rate cases are presented in the figure.

For each of the lowest three flow rate cases investigated (30, 54 and 116 mg/s), as typified by the 116 mg/s case shown in Fig. 2, the droplet emission rate was singly periodic. The corresponding autocorrelation functions exhibited distinct peaks at the mean periods and multiples thereof, as expected for singly periodic behavior. The values of the mean periods decreased with increasing flow rate. The period histograms were gaussian-like and unimodal, with a standard deviation that decreased with increasing flow rate (from 15 to 11 to 7 ms). These standard deviations were 4.4%, 5.4% and 6.1% of the mean period values, respectively, which were all greater than the measurement uncertainty in the period. This not only implied an increase in the percentage standard deviation with respect to the mean with increasing flow rate in the singly periodic regime, but also suggested that a stochastic element is present in this apparently deterministic problem. Even though the mass flow rate is kept constant, the periods and, by implication, the droplet volumes are not exactly the same each time, but vary within a 5% range.

Distinctly different patterns in the T_n vs. T_{n+1} diagrams, autocorrelation function and periodic histograms, however, emerged with a further increase in flow rate. At 157 mg/s, initial evidence of a period bifurcation was present. From observations, this appeared to be the premature and rather infrequent release of a droplet from the orifice temporally interspersed among a regular periodic droplet release. On the T_n vs. T_{n+1} diagram, this was characterized by a majority of period values clustered around 85 ms (the primary period)

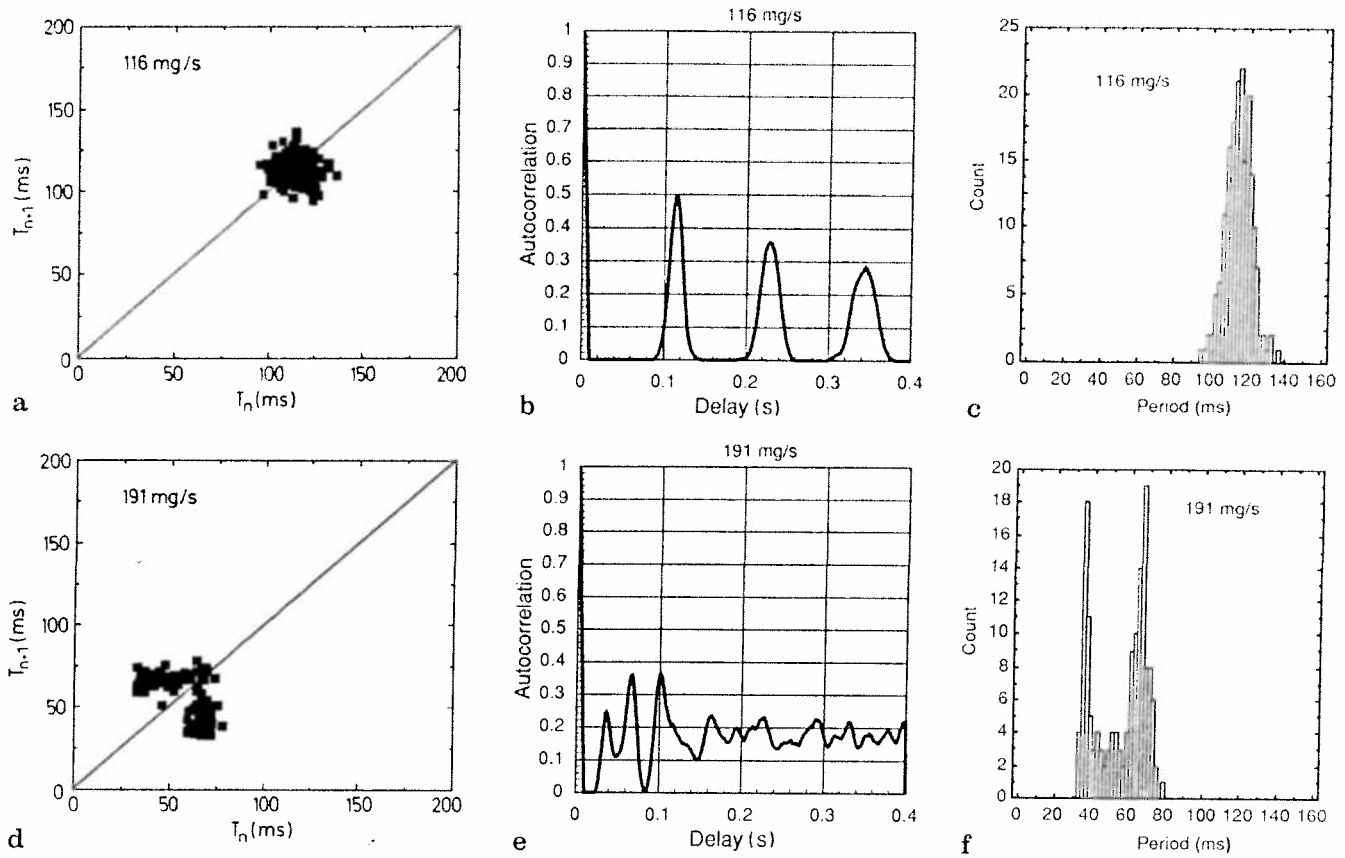

Fig. 2a–f. Single orifice data: T_n vs. T_{n+1} diagrams, autocorrelation functions, and period histograms for the 116 and 191 mg/s cases

and a few at approx. 40 to 55 ms, appearing as two tails extending from the main cluster. Here, it is important to note that period doubling would appear on the T_n vs. T_{n+1} diagram as two period clusters formed equidistant from the 45° line. The periods of the data in these tails appeared as slight bumps at the base of the corresponding autocorrelation function, at values equal to approximately one-half the primary period and whole multiples thereof. The corresponding period histogram revealed a relatively narrow distribution and two events occurring at approximately one-half the primary period. These trends in the T_n vs. T_{n+1} diagram, autocorrelation function and period histogram were accentuated further upon a flow rate increase to 166 mg/s.

At a mass flow rate of 191 mg/s (see Fig. 2), period doubling was much more evident, with two characteristic period clusters established at 35 and 67 ms, as displayed on the T_n vs. T_{n+1} diagram and in the period histogram. This was observed as the regular and sequential release of a droplet from the orifice followed, in almost an equal number of instances, by the release of a second, smaller droplet. The corresponding autocorrelation function was marked by the appearance of several peaks of somewhat equal but reduced value. These peaks represent the primary and doubled periods and multiples thereof. This is in contrast to the autocorrelation functions of the lower flow rate cases, which predominantly displayed one period with a high autocorrelation value and its multiples. At the highest mass flow rate examined (210 mg/s), this period doubling developed further showing two distinct clusters with slightly reduced periods (at approx. 32 and 59 ms). Full period doubling, as would be characterized by the disappearance of the primary period and the presence of only the doubled period, however, did not occur. The autocorrelation function had less pronounced peaks; the period histogram revealed the further progression toward the predominance of the doubled period.

Based upon the observation of two apparent sizes of droplets for the period-doubled case, the relation between droplet period and size was investigated in further detail by obtaining high-magnification video cassette recordings of the emitted droplets. This was done using orifice A and a mass flow rate of 185 mg/s, which was one of the lowest flow rates at which period doubling clearly was evident. The resulting period histogram for this case revealed two distinct periods at approx. 36 and 64 ms. A corresponding droplet volume histogram constructed from the measured droplet diameters displayed two characteristic volumes. This finding supported that period doubling was commensurate with the formation of droplets with volumes that were distinctly smaller than the primary droplets. As the extent of period doubling developed, more and more of these secondary droplets became interspersed temporally between the primary droplets.

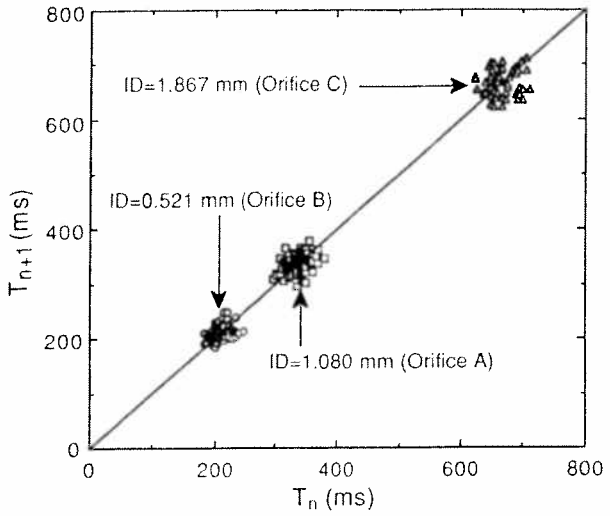

Fig. 3. The T_n vs. T_{n+1} diagrams for variable orifice IDs at 30 mg/s

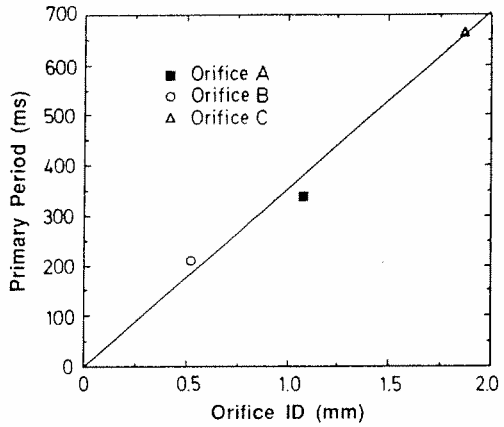

Fig. 4. Primary droplet emission period versus orifice ID at 30 mg/s

4.2 Effect of variable orifice diameter

Two further experiments were conducted at the lowest flow rate examined (30 mg/s) using orifices B and C. The resultant T_n vs. T_{n+1} diagram for all three orifices is given in Fig. 3. All three cases were singly periodic, as evidenced by their clustering about the 45° line. The dependency of the primary period on orifice ID was examined further. The results, as shown in Fig. 4, reveal that the primary period was correlated with ID to within 10% by the linear relation T(ms)= 350 D(mm), in which T denotes the period between successive drops and D the orifice ID. Thus, at a given mass flow rate in the singly periodic regime, the droplet size could be controlled through the choice of the orifice ID.

5 Double orifice experiment results and discussion

A series of eight experiments were performed using two type A orifices in which the effects of the total mass flow rate to the reservoir and common reservoir volume were investigated. Five of these were conducted using reservoir I and of the remaining three using reservoir II. Two additional experiments were performed in which the emitted droplets were recorded on video cassette under high magnification to compare measured and predicted droplet diameters.

5.1 Effect of mass flow rate

Five different total mass flow rates over the range of 140 mg/s to 260 mg/s were selected for this experiment using the smaller reservoir volume. The resulting temporal records were analyzed using the same methods as presented before, with the addition of determining the cross-correlation function of the period data of the two interconnected orifices. The results of two (224 and 264 mg/s) of the five cases examined are shown in Fig. 5. These two cases respectively represent the situations before and after period doubling in one of the orifices. The return map, auto- and cross-correlation functions for each of these two flow rate cases are presented in the figure.

For the two lower flow rates investigated (140 and 191 mg/s) both orifices exhibited singly periodic behavior, each with approximately the same characteristic period as the other, as shown by their T_n versus T_{n+1} diagrams. When the flow rate was increased to 224 mg/s (see Fig. 5), one orifice (A-1) began to exhibit a period bifurcation, while the other orifice (A-2) did so only very slightly and remained primarily singly periodic. For the remaining two highest flow rates examined (237 and 264 mg/s), as typified by the 264 mg/s case shown in Fig. 5, the extent of the period bifurcation for orifice A-1 developed further. Orifice A-2, however, returned to being singly periodic with a very distinct primary period. Data were not acquired beyond 264 mg/s, but some qualitative observations were made. Orifice A-1 remained doubly periodic as the flow rate was increased further. Orifice A-2, on the other hand, continued to remain singly periodic. Only at a relatively high flow rate through the reservoir (approx. 400 mg/s) did orifice A-2 again begin to exhibit a period bifurcation. At this point, the flow through orifice A-1 became a steady stream of liquid. These findings implied that at the flow rate favorable for initial period doubling through both orifices, period doubling occurred only for one orifice, which concurrently prevented the other orifice from period doubling.

The corresponding auto- and cross-correlation functions also are shown in Fig. 5 for the 224 and 264 mg/s cases. At the two lower flow rates, the autocorrelation functions show that both orifices were singly periodic. The cross-correlation functions reveal relatively mixed values over a range of delay times from zero to the primary period. The absence of dominant peaks indicated that there was no frequency- phase-locking between the two orifices. For the lowest flow rate case (140 mg/s), the cross-correlation value was unity at approx. 20 ms, which was 1/10th the primary period of orifice A-1. This implied that both orifices were in phase at approx. every tenth period with respect to orifice A-1. With a further increase in flow rate to 224 mg/s, both orifices began to under-

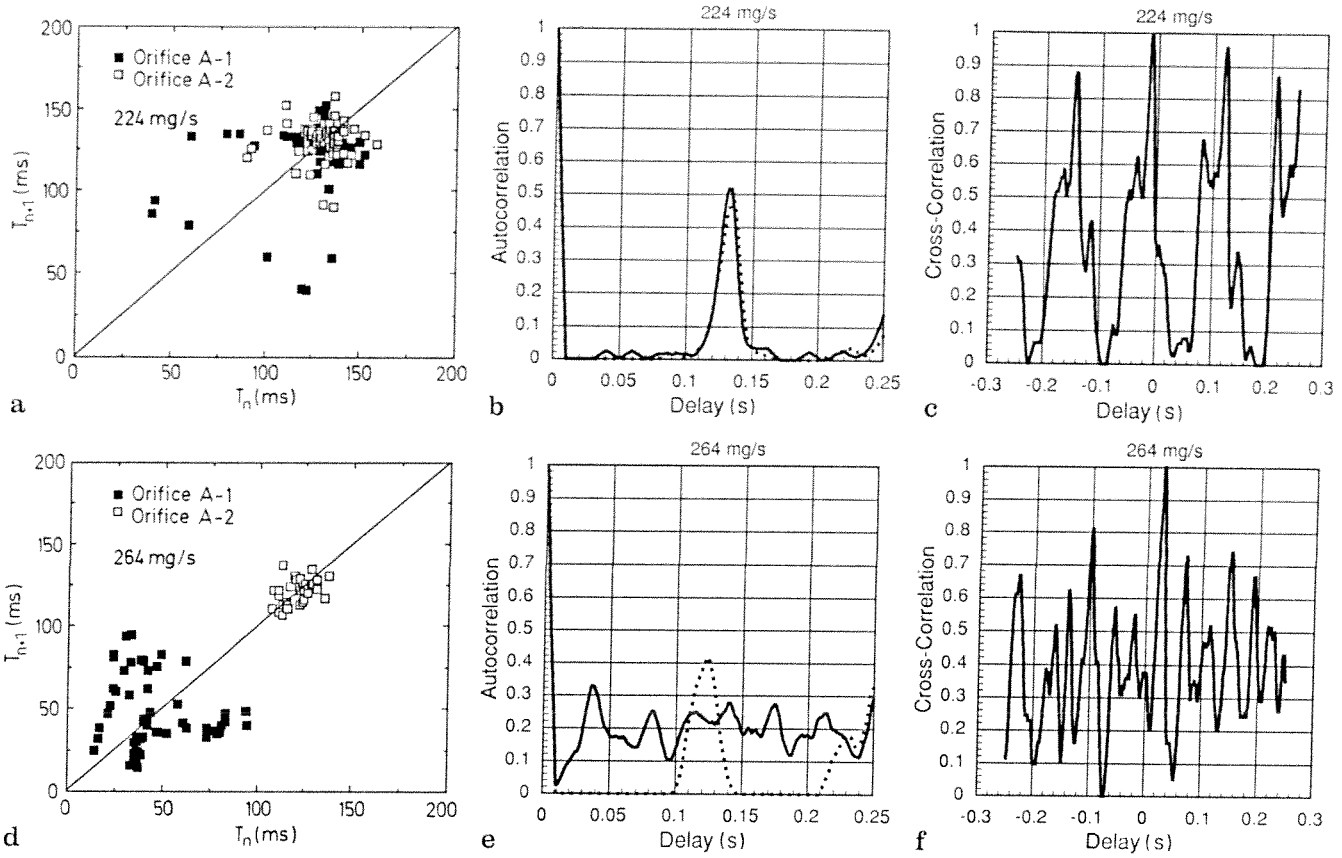

Fig. 5a–f. Small reservoir data: T_n vs. T_{n+1} diagrams, autocorrelation function and cross-correlation function for the 224 and 264 mg/s cases. Solid lines denote orifice A-1, dashed lines orifice A-2

go initial period bifurcation. Orifice A-1's autocorrelation function displayed relatively more bumps at its base as compared to orifice A-2, which corresponded to a greater number of doubled periods as noted previously in the T_n versus T_{n+1} diagrams. The cross-correlation function revealed very distinct peaks with near-unity values at delay times of approx. 20 ms with respect to the primary period value of 140 ms of either orifice. Thus, at approx. every seventh period, droplet emission from the orifices was in phase. This confirmed the observations made at this flow rate of in-phase dripping at every seventh droplet emission from orifice A-1.

When the flow rate was increased by approx. 5% to 237 mg/s, the period doubling of orifice A-1 developed further. Orifice A-2, however, reverted back to singly periodic behavior, as evidenced by distinct peaks in the autocorrelation function and a very narrow period distribution about the 45° line in the corresponding T_n vs. T_{n+1} diagram. The cross-correlation function was marked by a relatively elevated baseline and a value of unity at a delay time of 240 ms. This is approx. twice the value of the primary period of orifice A-2. At the highest flow rate examined (264 mg/s), the same trends for both orifices continued. The period doubling from orifice A-1 developed to a greater extent; orifice A-2 remained singly periodic, but showed some evidence for initial period doubling in the autocorrelation function.

5.2 Effect of reservoir volume

Three different total mass flow rates over the range of 128 mg/s to 306 mg/s were investigated using the larger reservoir volume. Only at the highest flow rate studied did droplet emission show any evidence of period doubling. The resultant T_n versus T_{n+1} diagrams and the corresponding auto- and cross-correlation functions for two (128 and 306 mg/s) of these three cases are shown in Fig. 6.

Both orifices exhibited singly periodic droplet emission at the two lower flow rates (128 and 216 mg/s). Their autocorrelation functions revealed rather distinct peaks at the primary periods. At 128 mg/s, the primary periods of droplet emission differed by approx. 10% due to a slight mismatch in their flow rates. This difference was reduced at higher flow rates. The cross-correlation function value at 128 mg/s was unity at approx. 40 mg/s, which was 1/5th the primary period of orifice A-1, implying that both orifices were in phase at approx. every fifth period with respect to orifice A-1. Similarly, a phase difference of ten orifice A-1 droplet periods occurred at 216 mg/s. At the highest flow rate (306 mg/s), there was evidence for initial period doubling in both orifices, as indicated by their autocorrelation functions. The corresponding cross-correlation function showed an in-phase delay time of approx. 45 ms.

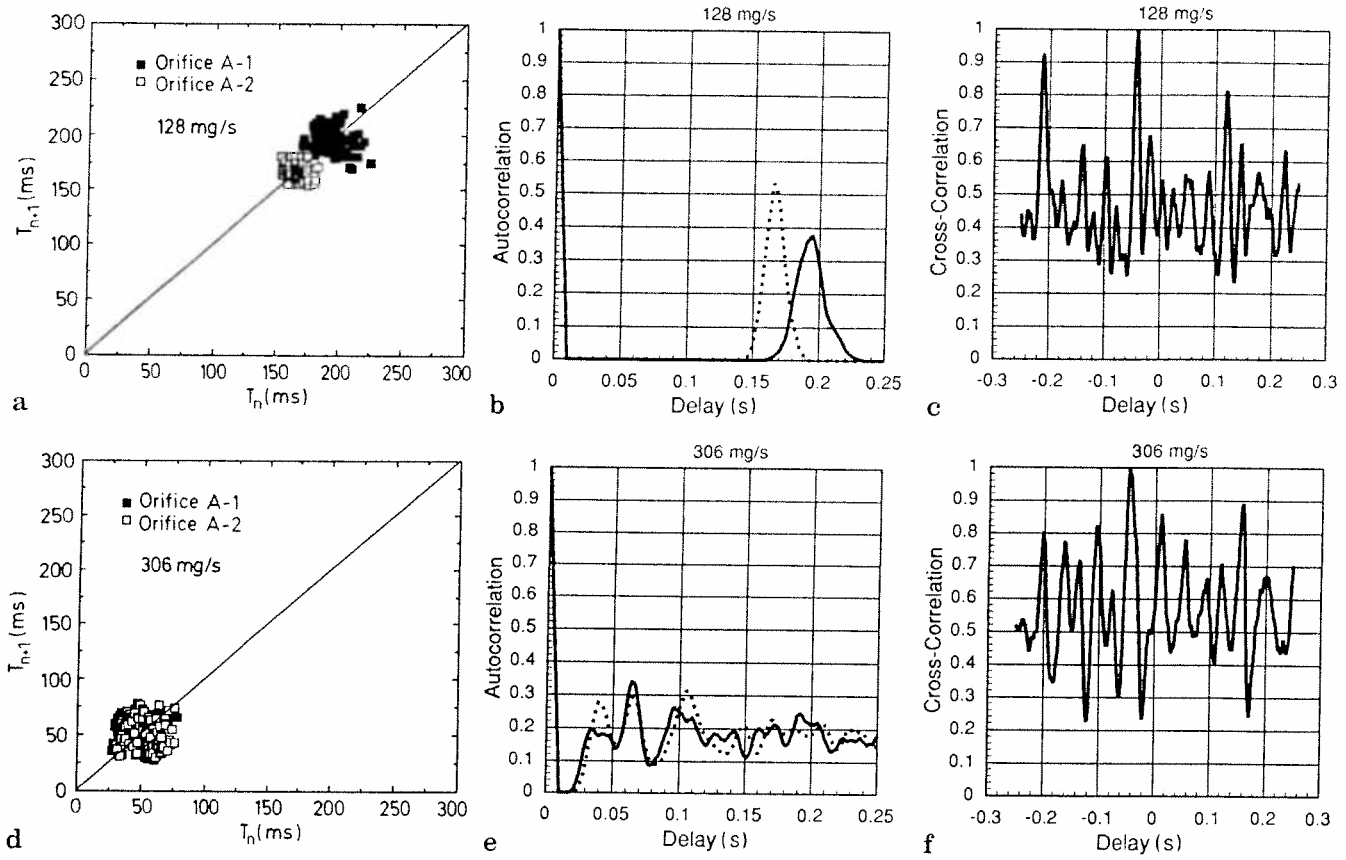

Fig. 6a–f. Large reservoir data: T_n vs. T_{n+1} diagrams, autocorrelation function and cross-correlation functions for the 128 and 306 mg/s cases. Solid lines denote orifice A-1, dashed lines orifice A-2

6 Comparison between single and double orifice experiment results

The periodicity of droplet production was examined in another context. The modal periods, i.e., those periods corresponding to the peaks of the distribution curves, first were determined from the period histograms. As displayed in Fig. 2. one distinct mode could be identified for the singly periodic cases and two for the doubly periodic ones. The resultant modal periods were plotted versus the mass flow rate to display more clearly the observed period bifurcation, as shown in Fig. 7. For the single orifice, the modal period between the emitted droplets was relatively high at the lower flow rates. The period then fell rapidly as the mass flow rate increased until, at 157 mg/s, a period bifurcation initiated. Thereupon, two characteristic modal periods emerged, which were similar to those reported in the dripping faucet experiments of Wu and Schelly (1989).

Similarly, the resultant modal periods for both the small and large reservoir cases were determined. As presented in Fig. 7 for the small reservoir I, orifice A-1 began to undergo a period bifurcation at 224 mg/s. This period doubling developed further at 264 mg/s where one modal period was approximately one-half the other (39 versus 79 ms). In contrast, for the large reservoir II, there was only initial period doubling at the highest flow rate investigated (306 mg/s). Hence, the most notable difference between the two reservoir volume cases was that the smaller reservoir volume yielded period doubling at a lower total mass flow rate.

Based upon these findings and those of the video recordings of the droplet formation process, a simple force balance model was developed. In these recordings, the emerging fluid was seen to accumulate at the tip of the orifice as a pendant mass. This pendant gradually grew in volume and progressively formed a neck between itself and the orifice. In time, this neck narrowed and, eventually, when the pendant liquid's weight could no longer be supported by the surface tension force at the neck, a droplet fell free. The remaining liquid retracted and the process began again.

The experimental observations suggested that the process of droplet emission in the present experiments was a "quasi-static" situation in which the surface tension and gravitational forces predominantly governed the droplet formation process. This was noted by an order of magnitude analysis of the ratios of forces involved. The forces considered are surface tension (σD), gravitational ($\varrho D^3 g$), inertial ($\varrho U^2 D^2$) and viscous ($\mu U D$) forces, where ϱ and σ are the fluid density and surface tension coefficient, respectively, D is the droplet diameter, g is the acceleration due to gravity, and $U = \dot{m}/\varrho D^2$ is the fluid velocity corresponding to the mass

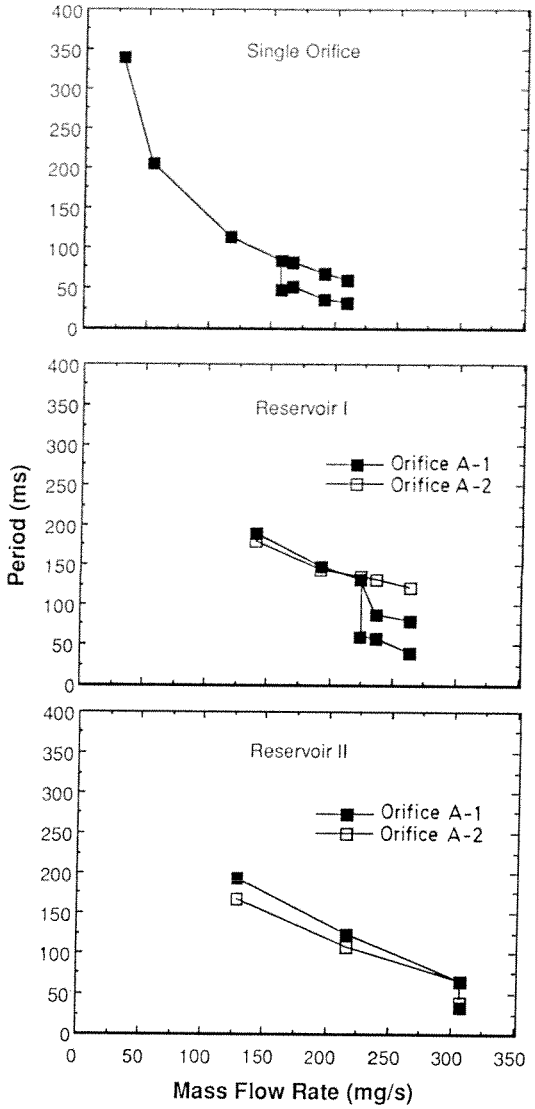

Fig. 7. Droplet emission modal period versus mass flow rate for single-orifice, and small reservoir and large reservoir double-orifice cases

flow rate. The ratios are the Bond number, $Bo = \varrho g D^2/\sigma$ (gravitational to surface tension), the capillary number, $Ca = \mu U/\sigma$ (viscous to surface tension), and Weber number, $We = \varrho U^2 D/\sigma$ (inertial to surface tension). The order of magnitude of these nondimensional groups are shown in Table 1 for this experiment and also for some other related studies in the literature.

Even though the data are from a variety of fluids, orifice diameters and flow rates, the surface tension and gravitational forces were comparable in all cases, being many orders of magnitude greater than inertial and viscous forces. From this, it appears that fairly simple modeling based on a static balance of forces can be used for the constant mass flow rate situation. This point of view is in contrast to that of Wilson (1988), who presented a detailed analytical model that included inertial and viscous forces. However, his experiments

Table 1. Order of magnitude of forces

Author	Bo	Ca	We
Harkins and Brown (1919)	1	10^{-10}	10^{-11}
Rayleigh (1899)	1	10^{-9}	10^{-10}
Wilson (1988)	1	10^{-3}	10^{-8}
Present work	1	10^{-6}	10^{-5}

did not verify his model probably because they were conducted at conditions where inertial and viscous forces did not dominate the surface tension force. Here, we assume that the weight of a droplet at departure under "quasi-static" equilibrium conditions can barely be sustained by the surface tension force, from which we have

$$\pi D \sigma F = \varrho g V_d \tag{3}$$

where V_d is the volume of a single drop, $\varrho = 789\ \mathrm{kg/m^3}$, $\sigma = 0.02275$ N/m, and F is a function of the geometry of the orifice's tip, the liquid's surface tension and density, and the emitted droplet size through the pendant's angle of curvature just prior to detachment. An exact expression, at present, to determine F is not known. This is primarily because of the few experiments conducted under constant mass flow rate conditions. As reported by Manfré (1966), the analogous values for F for a hydrostatically driven system range from 0.59 to 1.00.

For a spherical drop, the diameter d of the drop is given by

$$d = \left(\frac{6 D \sigma}{\varrho g}\right)^{1/3} \tag{4}$$

and the mass flow rate, $\dot{m}$, by

$$\dot{m} = \frac{\varrho V_d}{T}. \tag{5}$$

Using equation (3), we get

$$\dot{m} = \left(\frac{\pi D \sigma F}{g}\right) \frac{1}{T}. \tag{6}$$

This equation implies that for a fixed mass flow rate the period is proportional to the orifice ID.

This analysis was confirmed by several experiments. Equation (5) was verified through measurements of the mass flow rate, period and droplet diameter in two experiments, each using a different reservoir volume. Equation (6) was used to determine F based upon all of the singly periodic data obtained in these experiments and then to verify the inverse proportionality between mass flow rate and period.

In the two experiments conducted to verify Eq. (5), the emitted droplets were recorded on video cassette under high magnification to compare measured and predicted droplet diameters. Singly periodic droplet emission rates were obtained using reservoir I at a mass flow rate of 110 mg/s and reservoir II at 66 mg/s. The 110 mg/s case had a primary

period of 163 ms and a measured droplet diameter of 2.76 mm; the 66 mg/s case correspondingly 109 ms and 3.01 mm. The resultant droplet diameters computed using Eq. (5) were 3.07 and 2.96 mm, respectively. This yielded percent differences between the measured and calculated diameters of 10% and 1.7%, respectively. These results not only confirmed that the measured and calculated diameters agreed to within 10%, but also that the diameter of the droplets for a fixed orifice diameter was invariant within this band before period doubling occurs. That is, as the mass flow rate was increased in the singly periodic regime, the additional mass was ejected from the orifice by increasing the rate at which the droplets were produced rather than by increasing the size of the droplets with their production rate fixed.

The proposed inverse proportionality between mass flow rate and period, as given by Eq. (6), was verified and the function F was determined through further examination of all singly periodic data obtained in either the single or double orifice experiments. Because of the slight mismatch in the mass flow rates between the two orifices, the mass flow rate of each individual orifice was measured. The resultant primary period was plotted versus the mass flow rate per orifice, as displayed in Fig. 8. The results verified the inverse proportionality between mass flow rate and primary period, as shown in the figure by the very good agreement between calculated and experimental results with F equal to 1.5 in Eq. (6). The scatter of the data from the single and double orifice cases about this simple fit of the data (which was approx. 10% at maximum) additionally implied that the reservoir volume did not effect the period of droplet emission at a fixed mass flow rate and orifice diameter.

The individual orifice flow rate acquired for both the single and double orifice cases also was used to determine the incipient mass flow rate for period doubling and its relation to reservoir volume size. As noted previously, initial period doubling for the single orifice occurred at approx. 160 mg/s. The corresponding mass flow rate per orifice for each of the small and large reservoirs was determined to be approximately 100 and 150 mg/s, respectively. Here, the incipient mass flow rate per orifice for period doubling for the larger reservoir case more closely approximated that of the single orifice case, whereas that for the smaller reservoir case was lower. This directly supports the assertion that increases in the reservoir volume lead to increases in the incipient mass flow rate per orifice for period doubling close to the upper limit of the single orifice case. In this light, any increase in the reservoir volume would eventually lead to the periodic droplet emission behavior of a single orifice. It also can stated that relatively small reservoir volumes allow for inter-orifice interaction such that the onset of period doubling from one can directly affect the periodic behavior of the other.

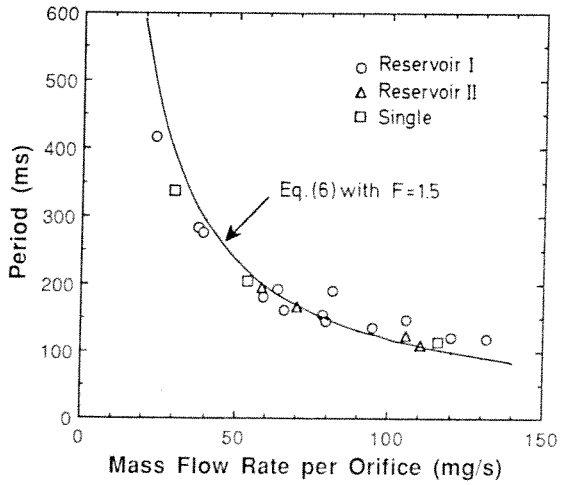

Fig. 8. Singly periodic droplet emission modal period versus individual orifice mass flow rate per orifice

7 Conclusions

Although the formation and emission of droplets have been studied for a long time, there is as yet no comprehensive theory that can predict either the dripping frequency or the dynamics of the period doubling bifurcation from a single orifice driven either hydrostatically or under constant mass flow rate conditions. A major factor for this is that the interplay between surface tension and gravitational forces is complicated by the shape of the pendant's neck curvature at the instant of release. This curvature implicitly is governed by the dimensions of the orifice and droplet, and by the liquid's surface tension and density. As a consequence, it is found that it is not possible to collapse all experimental data into a single curve for either type of driven system simply by using one nondimensional parameter.

The experimental results reported herein indicate that dripping from an individual orifice at relatively low mass flow rates is singly periodic and that the period between droplets is inversely proportional to the imposed mass flow rate. The relatively large scatter of the period data in this regime suggests that a stochastic element is present in this apparently deterministic problem. The experimental data are consistent with a model in which the droplets of the same diameter are formed by the interplay between surface tension and gravitational forces, and emanate at a rate related to the orifice's mass flow rate. As the mass flow rate is increased, smaller diameter droplets, interspersed temporally among the primary droplets, are formed. These droplets are responsible for the period doubling. Further increases in the mass flow rate yield an increase in the smaller diameter droplet population.

The presence of a common fluid reservoir volume between two orifices of the same diameter does not affect the droplet emission rate in the singly periodic regime of either orifice as compared to its single orifice counterpart. However, the volume of the reservoir does affect the mass flow rate per orifice necessary for initial period doubling, with this

critical mass flow rate being lower for a smaller reservoir volume. This consequently implies that care must be taken to prevent the behavior of droplet emission from one orifice affecting that from the others when designing configurations in which multiple orifices are interconnected through a common reservoir.

Acknowledgements

We acknowledge the financial support of D. M. Weis during the summer of 1990 through the National Science Foundation – Research Experience for Undergraduates Program (#EIO 90-00675).

References

Asai, A. 1989: Application of the nucleation theory to the design of bubble jet printers. Jap. J. Appl. Phys. 28, 909–915

Crutchfield, J. P.; Farmer, J. D.; Packard, N. H.; Shaw, R. S. 1986: Chaos. Sci. Am. 255, No. 6, 46–57

Harkins, W. D.; Brown, F. E. 1919: The determination of surface tension (free surface energy), and the weight of falling drops: The surface tension of water and benzene by the capillary height method. J. Am. Chem. Soc. Vol. XLI, 499–524

Manfré, G. 1966: Rheological aspects of drop formation. J. Appl. Phys. 37, 1955–1962

Martien, P.; Pope, S. C.; Scott, P. L.; Shaw, R. 1985: The chaotic behavior of the leaky faucet. Phys. Lett. 110A, 399–404

Padday, J. F.; Pitt, A. R. 1973: The stability of axisymmetric menisci. Philos. Trans. R. Soc. London 275, No. 1253, 489–528

Rayleigh, Lord 1899: The size of drops. Philos. Mag. 48, No. 293, 321–337

Shaw, R. 1984: The dripping faucet as a model chaotic system. Santa Cruz: Aerial Press

Tate, T. 1864: On the magnitude of a drop of liquid formed under different circumstances. Philos. Mag. J. Sci., Vol. XXVII, 4th Series, 176–180

Weis, D. M.; Dunn, P. F.; Sen, M. 1991: The single and double periodicity of droplets emanating from interconnected orifices. Report No. UND/HCAR/PDL/DW-91-1, Hessert Center for Aerospace Research, University of Notre Dame, Notre Dame, IN

Wilson, S. D. R. 1988: The slow dripping of a viscous fluid. J. Fluid Mech. 190, 561–570

Wu, X.; Schelly, Z. A. 1989: The effects of surface tension and temperature on the nonlinear dynamics of the dripping faucet. Physica D 40, 433–443

Received November 25, 1991